Correlation between Sub-Tg relaxation processes and mechanical behavior for different hydrothermal ageing conditions in epoxy assemblies

Mathieu Chevalier, Eric Dantras, Claire Tonon, Pascale Guigue, Colette Lacabanne, C. Puig, Christian Durin

DOI 10.1002/app.31253

Correlation Between Sub-T_g Relaxation Processes and Mechanical Behavior for Different Hydrothermal Ageing Conditions in Epoxy Assemblies

M. Chevalier,[1] E. Dantras,[1] C. Tonon,[2] P. Guigue,[3] C. Lacabanne,[1] C. Puig,[2] C. Durin[3]

[1]*Laboratoire de Physique des Polymères, Institut Carnot CIRIMAT, Université Paul Sabatier, Toulouse Cedex 31062, France*
[2]*Astrium, 31 avenue des Cosmonautes, Toulouse 31402, France*
[3]*Centre National d'Etudes Spatiales, 18 avenue Edouard Belin, Toulouse 31401, France*

ABSTRACT: The aim of this study is to understand aging phenomena by monitoring physical parameters after real and simulated aging experiments. This study focuses on aluminum-epoxy assemblies, which are commonly used on spacecraft structures. Different samples are submitted to simulated aging tests. Influence of temperature and moisture is analyzed. Evolution with aging is characterized at two different scales. The macroscopic behavior of the assemblies is studied by single lap shear test. A decrease in the shear rupture stress is observed with increasing temperature and relative humidity. It is demonstrated that temperature has more important influence. The molecular behavior in the adhesive joint is studied by dynamic dielectric spectroscopy measurements. This experiment gives access to molecular mobility in the adhesive. Dipolar entities are identified as evolving with aging conditions. The temperature is more effective than moisture at this scale. An interpretation of the molecular mobility before and after aging shows that water is an important parameter of this study. A link between mechanical and molecular behavior with hydrothermal aging is found. The decrease of mechanical properties occurs while failures become interfacial. In the same time, the interactions between hydroxyether and water increase. The evolution of the macroscopic behavior of the bonded assemblies is due to this combination observed at different scales.

Key words: epoxy; adhesive; dielectric spectroscopy; aging; single lap shear

INTRODUCTION

Aging processes in materials used for space applications depend on various parameters (on ground and space environments) and are not fully understood. The influence of each factor remains obscur. A particular attention shall be paid on the aging of bonded assemblies due to storage on ground and thermal cycling in orbit.

During spacecraft integration, in clean room, materials are used under humid and thermal controlled conditions: 21 ± 2°C, 50 ± 5%RH. The integration activities and the storage can last several years. Consequently, it is necessary to take into account the time spent in clean room as an aging factor. An aging process, which begins before the launch could be the cause of an irreversible damage during the flight. All the structures of the satellite are submitted to these controlled environmental conditions. The characterization and the simulation of aging phenomena in bonded assemblies are the challenge to improve their conception and their durability. Checking these assemblies after the launch is impossible. One alternative is to use accelerated testing on the basis of space industry knowledge and ESA normative data.[1] Empirical laws are the only way to obtain accelerated aging conditions. But, the link between accelerated testing and real-time aging is unknown. The aim of this study is to shed some light on this correlation.

The methodology used for the work presented later is to carry out an investigation of the mechanical behavior and molecular dynamics evolutions in thermoset bonded structures exposed to moisture. The combined use of mechanical and dielectric measurements has been chosen to evaluate epoxy–water interactions at macroscopic and molecular scales.

Epoxy–amine networks are relatively hydrophilic materials. They are able to absorb 1–6% per weight of water in many industrial formulations.[2] Numerous studies have been devoted to the water

Correspondence to: E. Dantras (dantras@cict.fr).

absorption process in these systems but this problem remains only partly understood.[2–6] Water ingress in polyepoxy networks leads to a range of effects[3]: bulk dissolution by water in the polymer network, moisture absorption on the surface of free volume holes in the glassy structure, interaction of water with hydrophilic polar moieties, such as amines and hydroxyls by strong hydrogen bonds. It is also reported that water is present in two different forms in polyepoxy networks[4,7–9]: free water that fills the microvoids of the network and bound water that bonds with polar groups.

A decrease in mechanical properties of bulk and bonded polyepoxy networks, such as modulus and rupture strength under humid conditions is observed. It is related to plasticization.[9–11] But how absorbed water affects the mobility of polymer chains is not well known. According to Mijovic et al.,[5] the chemical and physical changes on the molecular level during the early stage of environmental exposure is the most important point in the prediction of performance in adhesive joints.

The use of dynamic mechanical and dielectric measurements allows us to investigate the molecular dynamics. In polyepoxy systems, two to four relaxation regions have been reported by different experimental techniques.[12–16] Some authors studied the influence of water on molecular dynamics of amine cured epoxy adhesives.[5,8,10,12] They reported that some relaxational processes were influenced by the ingress of water into the network. But some results are contradictory, probably due to the complexity of the commercial adhesive formulations.

Therefore, the main objective of this study is to get a simultaneous evaluation of macroscopic and molecular changes in bonded structures exposed to hydrothermal environment.

EXPERIMENTAL

Materials

The studied system is an aluminum-epoxy assembly. The adhesive is a commercial amine-epoxy bicomposant adhesive packaged to be usable immediately. The two parts are prepared and a nozzle allows us to make and extrude the mix with an accurate repeatability. The hardener (part A) is a mix of several components, where aliphatic amine is preponderant. The part B is based on diglycidyl ether of bisphenol-A epoxy resin mixed with other components (fillers, catalyst…). Parts A and B are mixed at room temperature (ratio 2 : 1). The curing process is 7 days at 21 ± 2°C, 50 ± 5%RH. It leads to two glassy transitions (T_g) determined by Diathermal Scanning Calorimetry measurements. One, equal to 60°C, is associated with the high-crosslink network. The second one, equal to 10°C, corresponds to the low-crosslink regions. Both substrates are wrought aluminum alloys (2024 or 2017) widely used in aerospace industry. By this way, differential thermal expansions (ΔCTE) between the two substrates are avoided. This assembly is considered as a model. The joint thickness is ranging from 70 to 200 μm.

Hydrothermal aging conditions

During accelerated hydrothermal aging tests, the joints are exposed to a warm humid environment during 7 days. The temperature range is from 20 to 80°C (step = 20°C) and the relative humidity is ranging from 20%RH to vapor saturation by steps of 20%RH. Each temperature–relative humidity pair is tested.

Methods

Single lap shear test

Single lap shear tests are performed at 25°C using the tensile tension machine Instron 4505 with a 100 kN load cell. The crosshead speed is 1 mm/min. Three specimens were studied for each test. Data were recorded with the Serie IX software. The ruptures were analyzed visually to determine the percentage of cohesive failure.

Thermo mechanical analysis

Thermo mechanical measurements are performed using an Advanced Rheometric Expansion System strain controlled rheometer (TA Instuments) in the torsion rectangular mode within the linear elasticity range. Dynamic mechanical storage and loss modulus G′ and G″ were recorded as function of temperature from −50 to 100°C at 3°C/min, for an angular frequency equal to 1 rad/s.

Dynamic dielectric spectroscopy

Broadband dielectric measurements are performed using a Novocontrol BDS 4000 covering a frequency range from 10^{-2} Hz to 10^{6} Hz with 10 points per decade. Experiments were carried out isothermally from −150 to 150°C by steps of 5°C. The temperature is controlled with an accuracy of ±0.5°C by a nitrogen gas stream heated by a Quatro temperature controller. The samples are round plate assemblies (Φ = 40 mm). We use the aluminum alloy substrates as electrodes.

The real ε′ and imaginary ε″ parts of the relative complex permittivity ε* are measured as a function of frequency f at a given temperature T. Experimental data are fitted by the Havriliak-Negami (HN)

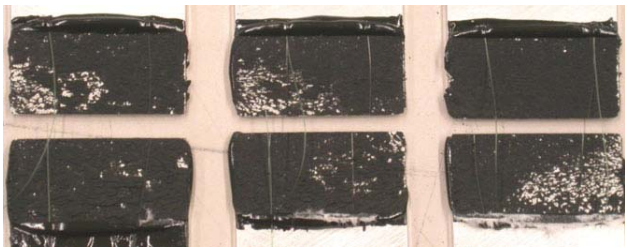

Figure 1 Fracture appearance for three single lap shear samples at initial state. [Color figure can be viewed in the online issue, which is available at www.interscience.wiley.com.]

[eq. (1)] function with an additional conductivity term.[17,18]

$$\varepsilon^*(\omega) = \varepsilon_\infty + \frac{(\varepsilon_s - \varepsilon_\infty)}{(1 + (i\omega\tau_{HN})^{\alpha_{HN}})^{\beta_{HN}}} + \frac{\sigma_0}{i\varepsilon_0\omega} \qquad (1)$$

where ε_∞ is the real permittivity for high frequencies, $\Delta\varepsilon$ is the relaxation strength, α_{HN} and β_{HN} are the HN parameters, τ_{HN} is the relaxation time, ω is the angular frequency, σ_0 is the d.c. conductivity, and ε_0 the dielectric permittivity of vacuum.

RESULTS

Mechanical behavior

Static mechanical behavior

The shear behavior is characterized at initial state. The shear rupture stress σ_R is 27.5 ± 0.3 MPa. The fracture appearance is cohesive as shown in Figure 1. The cohesive surface is 89 ± 1% of the bonded surface. These values are considered as reference values before aging.

Single lap shear tests are performed after different aging conditions. The shear rupture stresses are

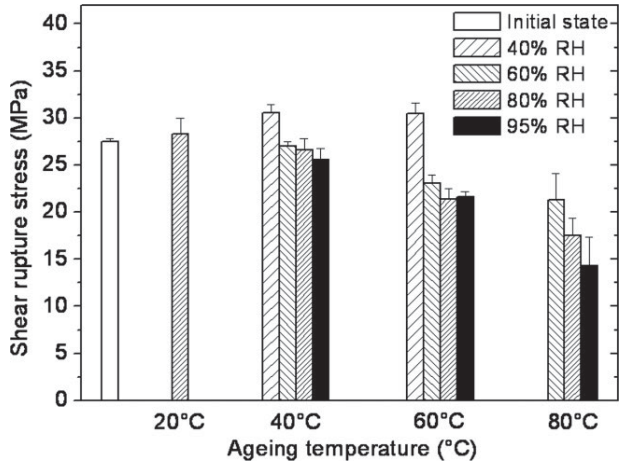

Figure 2 Evolution of the shear rupture stress as a function of temperature and humidity percentage.

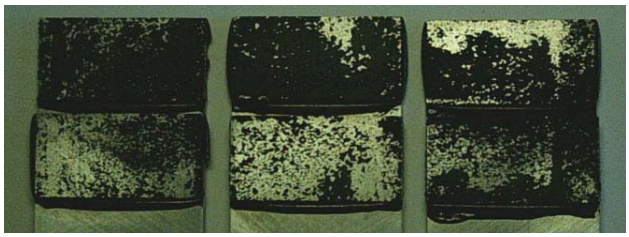

Figure 3 Fracture appearance for three single lap shear samples after 7 days under 80°C, 95%RH. [Color figure can be viewed in the online issue, which is available at www.interscience.wiley.com.]

shown in Figure 2 as function of aging temperature for different relative humidity percentage. First, we note that σ_R is higher than σ_R at initial state when the relative moisture percentage of the tests is 40%RH, i.e. lower than clean room conditions. For this moisture environment, σ_R value is independent of the aging temperature. For a given relative humidity percentage, σ_R exhibits a linear decrease as function of temperature. The influence of relative humidity is also analyzed. For isothermal aging conditions, a nonlinear decrease of σ_R is observed as function of moisture amount. The higher the temperature is, the higher the moisture influence.

The evolution of the failures is studied. Figure 3 shows the failure after aging at 80°C, 95%RH. The cohesive failure percentage is reported in the Table I. As function of increasing aging temperature and humidity, we note that the rupture becomes more interfacial. For 80°C and 95%RH aging conditions, we observe that the ratio between interfacial and cohesive failures is about one.

Dynamic mechanical behavior

The storage modulus G′ and loss modulus G″ are shown in Figure 4 as function of temperature for the bulk adhesive at initial state. The conservative modulus decreases from 1 GPa at −45–0.8 GPa at 40°C. From 50 to 80°C, the decrease is stronger. G′ reaches 10 MPa. This transition is associated with the mechanical manifestation of glass transition. The loss modulus exhibits two relaxation phenomena

TABLE I
Cohesive Failure Percentage as a Function of Hydrothermal Ageing Conditions

	Aging temperature (°C)			
Aging moisture (%RH)	20	40	60	80
40	N/A	87 ± 4	78 ± 3	N/A
60	N/A	77 ± 11	65 ± 12	79 ± 9
80	80 ± 2	75 ± 6	60 ± 4	61 ± 7
95	N/A	70 ± 11	61 ± 1	45 ± 7

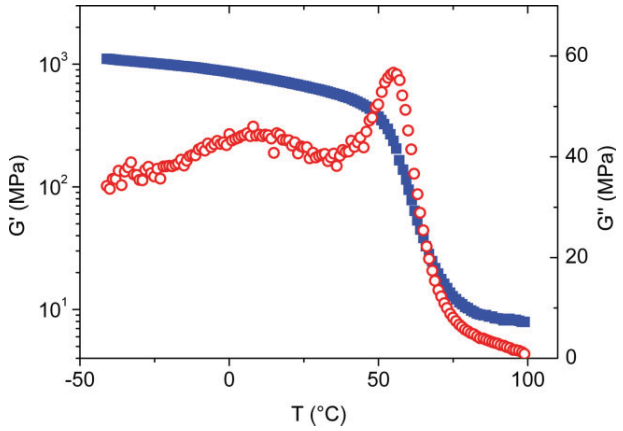

Figure 4 Storage modulus G′ (squares) and loss modulus (circles) as function of temperature for the bulk adhesive at initial state. [Color figure can be viewed in the online issue, which is available at www.interscience.wiley.com.]

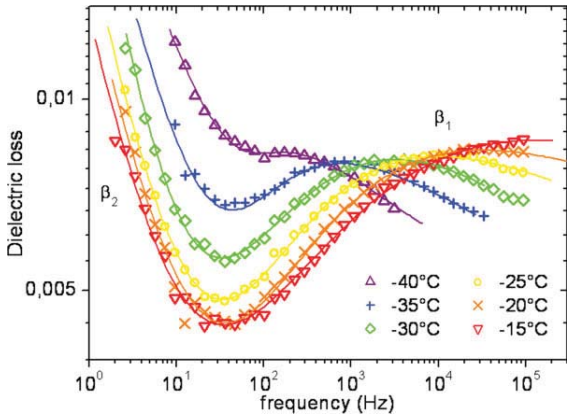

Figure 6 Isothermal dielectric loss at initial state as a function of frequency showing β1 relaxation. [Color figure can be viewed in the online issue, which is available at www.interscience.wiley.com.]

called ω and α. ω peak reaches a maximum at 10°C. This relaxation is associated with heterogeneities in the adhesive.[19] α reaches a maximum at T_α temperature equal to 55°C.

Dielectric behavior

Molecular mobility at initial state

The dielectric loss from −150 to 150°C of an assembly at initial state shown in Figure 5. Six dielectric phenomena are pointed out. In the low temperature range a weak and broad relaxation mode is observed, labeled γ. At higher temperature, a more intense and narrow atypical mode β_2 is found. Then, a weak and broad mode is detected: this mode is called β_1. The dielectric loss corresponding to this relaxation is shown in Figure 6 for temperatures ranging from −40 to −15°C. In the high temperature range, three additional relaxations occur: ω, α, and MWS modes.

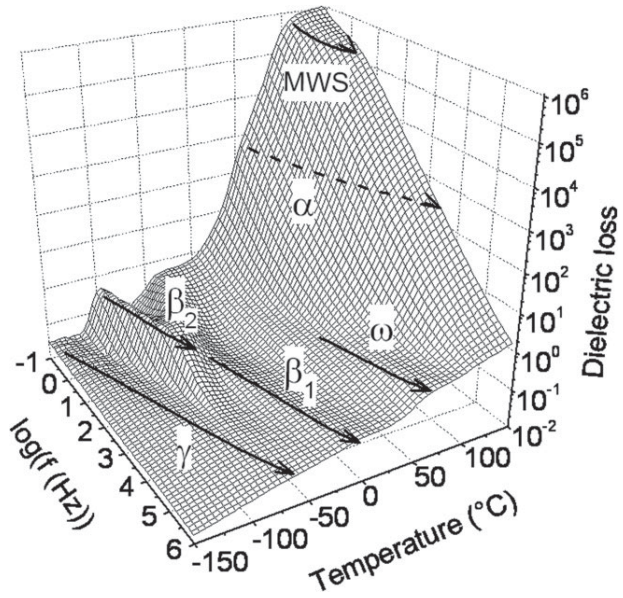

Figure 5 Dielectric loss at initial state reported on a logarithmic scale as a function of temperature and frequency.

Secondary relaxation modes have various molecular origins. The γ mode is related to the CH_2 mobility in aliphatic chain sequences.[12,13] The molecular origin of β_2 and β_1 is more complex. β modes are a combination of several molecular entities. According to Ochi et al.,[15] β is mainly associated with the mobility of hydroxyether and diphenyl propane groups. At higher temperatures, ω is associated with heterogeneities in the adhesive as observed previously during thermo mechanical measurements.[19] α is attributed to the dielectric manifestation of glass transition. The MWS relaxation is attributed to macrodipoles.

Relaxation times τ_{HN} are determined using the Havriliak-Negami function [eq. (1)]. The temperature dependence of γ, β_2, and β_1 relaxation times at initial state is reported in the Arrhenius diagram presented in Figure 7. The increase of dynamic dielectric spectroscopy (DDS) measurement temperature shows that γ, β_2, and β_1 modes follow an Arrhenius law as expected [eq. (2)].

$$\tau(T) = \tau_0 \exp\left(\frac{\Delta H}{RT}\right) \tag{2}$$

where ΔH is the activation enthalpy, τ_0 is the pre-exponential factor, and R is the universal gas constant.

The ω, α, and MWS evolution is more difficult to analyze. At high temperatures, conductivity appears. Consequently, the use of the HN equation is more complex: we observed a merging between high temperature relaxation modes and conductivity phenomenon. The behavior of these relaxation

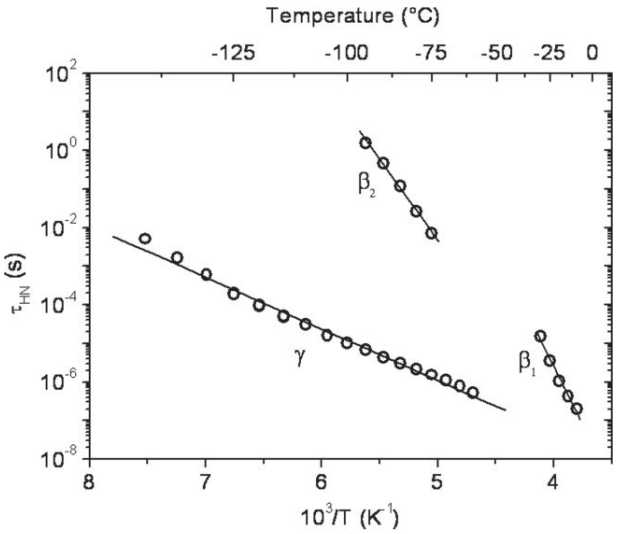

Figure 7 Relaxation times of γ, β_1, and β_2: experimental points (o) with Arrhenius fits shown by the solid lines.

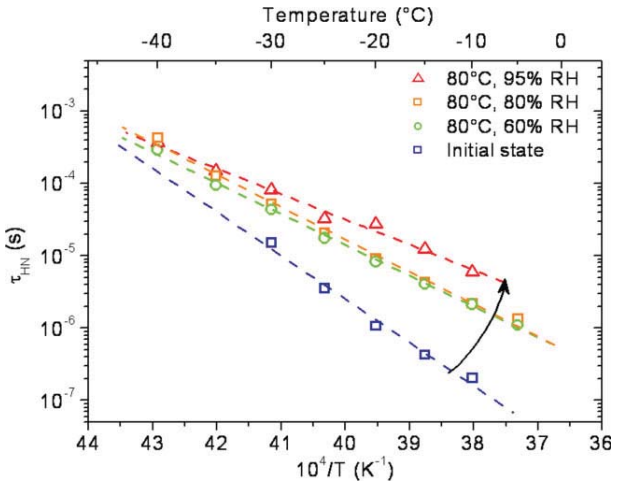

Figure 9 β_1 mode relaxation times after 80°C aging as a function of temperature. [Color figure can be viewed in the online issue, which is available at www.interscience.wiley.com.]

phenomena is not presented in this article. We will focus on the evolution of localized mobility associated with secondary relaxation modes as function of hydrothermal aging parameters.

Molecular mobility after aging

Hydrothermal aging induces an evolution in γ and β_1 behaviors. β_2 is not affected. For purpose of clarity, Figure 8 focuses on γ evolution with aging. The higher the aging temperature is, the higher the shift on γ. This change is the same for all moisture content performed at 60 and 80°C.

The evolution of β_1 relaxation times after hydrothermal aging is presented in Figure 9 after 80°C aging. β_1 relaxation times are unchanged in the low temperature range for each case. At 80°C, whatever the relative humidity conditions of the test, i.e. 60–95%RH, the relaxation times associated with β_1 are slower than at initial state.

The evolution of β_1 relaxation times after 80%RH is presented in Figure 10. At 80%RH, while the DDS temperature measurements increase, the relaxation times shift to higher temperature of 60 and 80°C aging temperatures. After 20 and 40°C aging temperatures, there is no evolution in β_1 relaxation times.

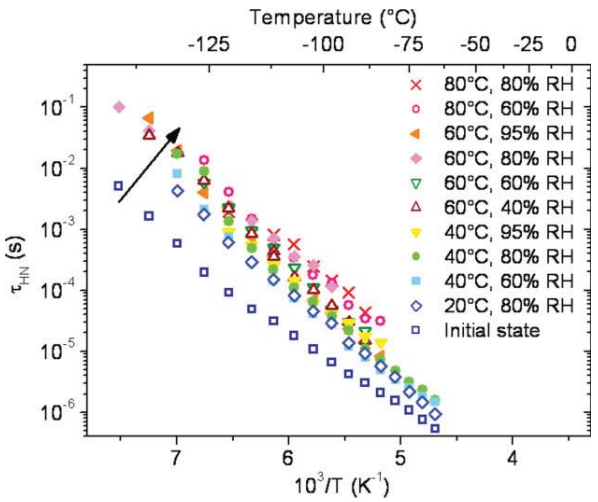

Figure 8 γ mode relaxation times as a function of temperature after hydrothermal aging. [Color figure can be viewed in the online issue, which is available at www.interscience.wiley.com.]

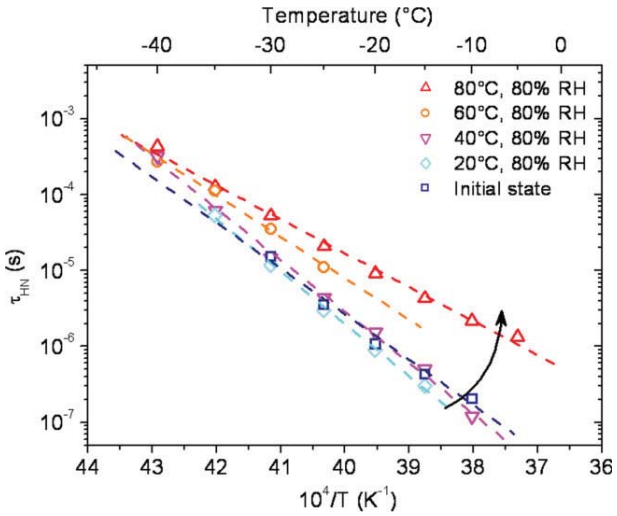

Figure 10 β_1 mode relaxation times after 80% RH aging as a function of temperature. [Color figure can be viewed in the online issue, which is available at www.interscience.wiley.com.]

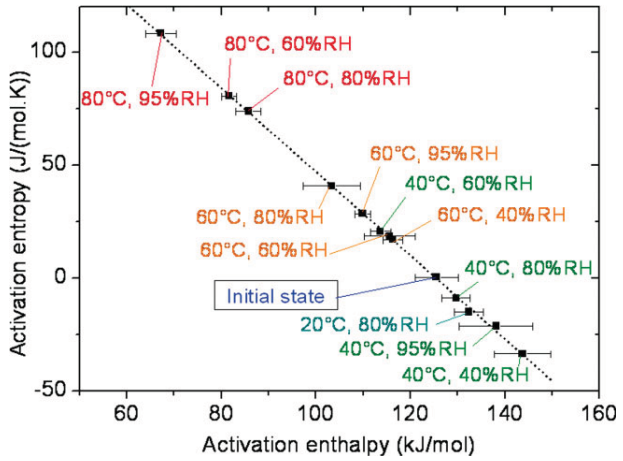

Figure 11 β_1 enthalpy–entropy compensation after hydrothermal aging conditions. [Color figure can be viewed in the online issue, which is available at www.interscience.wiley.com.]

Figures 9 and 10 show a compensation phenomenon at low temperatures. Whatever the aging conditions, τ_{HN} is equal to 10^{-3} s at −45°C. Similar behavior have already been observed for plasticizers in a polymer matrix.[20]

Activation enthalpy and pre-exponential factors are calculated from eq. (2). According to Eyring theory, eq. (3) gives the activation entropy.

$$\tau_0 = \frac{h}{kT}\exp\left(-\frac{\Delta S}{R}\right) \tag{3}$$

where h is the Planck constant, k is the Boltzmann constant, and ΔS is the activation entropy.

Activation entropy is reported as function of activation enthalpy on Figure 11. We observe a compensation phenomenon between ΔS and ΔH for each hydrothermal aging condition. When the aging temperature is 20 and 40°C, an increase in the activation enthalpy and a decrease in activation entropy compared to initial state was noted. At 60 and 80°C aging temperatures, the activation enthalpy shifts to lower values while the activation entropy increases. ΔS reaches a maximum for the most severe hydrothermal aging parameters.

DISCUSSION

Figure 2 shows that the temperature aging parameter is preponderant in the mechanical damage induced by hydrothermal tests. When the aging temperature increases, humidity appears more effectively. Such behavior is characteristic of a thermally activated phenomenon like diffusion. Water absorption into the joint is deeply linked to mechanical properties. Failure analysis reported in the Table I shows that interfacial rupture area increases when the aging conditions are more severe. These results coincide with Cognard approach.[21] Interfacial area could correspond to water clustering between the substrate and the adhesive. The point is emphasized by the slow decrease of the cohesive rupture area and σ_R after 40%RH aging whatever the temperature.

At molecular scale, change in γ behavior with aging is observed on the Figure 8. It is attributed to an annealing effect. Relaxation times associated with γ reach a maximum shift when the test temperature is maximum. ΔH is equal before and after aging. τ_0 increases. This evolution is explained by conformational defaults in aliphatic sequences due to polymerization. In the initial state, some epoxy and amine reactive groups remain into the polymer. They cannot react due to the network cohesion and the limited mobility corresponding to the glassy state. CH_2 mobility becomes slower with aging temperature. It traduces that conformational state along aliphatic sequences becomes thermodynamically more stable.

Relaxation times corresponding to β_1 are shown in Figure 9 and the Figure 10. The evolution of the mobility after aging traduces that around the hydroxyether entities, the physical environment is modified. The influence of aging temperature is pointed out. When the temperature is 60 and 80°C, whatever the humidity, we observed a decrease in the activation enthalpy and an increase in the activation entropy shown in Figure 11. It means an increase in disorder around hydroxyether moieties. When the aging temperature is 40°C, the opposite is observed traducing an increase of local order. The temperature treatment influence changes, as function of crossing T_α shown in Figure 4. Below T_α, the mobility is limited. Water diffusion is slightly activated. It leads to no evolution at localized scale around the hydroxyether entities. Above the mechanical manifestation of glass transition, the mobility is increased and the diffusion process is more activated due to temperature. The shift in the relaxation times is observed. Some authors observed that β relaxation modes evolve with increasing moisture.[5,8,16] They concluded that hydroxyether (i.e. hydrophilic entity)–water interactions occurs, modifying relaxation times. Though, they observed an increase in hydroxyether mobility when there is a increase in moisture into the joint. In our case, we note that the mobility decreases at high temperature when the hydrothermal aging conditions are more severe. The compensation between entropy and enthalpy also shows the local modification probably due to interaction with water. The loss in molecular mobility traduces this phenomenon. This mode can be used as a dielectrical marker to study hydrothermal effect in adhesive joint.

Correlation between mechanical and molecular changes

After 7 days of aging in different hydrothermal aging conditions, the studied adhesive exhibits a change in the shear behavior and in the mobility of hydroxyether entities. At macroscopic and molecular scales, we observe that the aging temperature is a more influent parameter than the aging relative humidity percentage. As the aging temperature increases, a decrease in shear rupture stress is denoted. This diminution corresponds to a decrease of hydroxyether mobility in the adhesive. The similarity of these two behaviors let us to think that the water present into the joint bonds with hydroxyether moieties by hydrogen bonds and play a role in diminishing mechanical properties. To complete this study, now we need to analyze the behavior of the α mode, with hydrothermal aging conditions, i.e. at a delocalised scale in the network. The evolution of the dielectric manifestation of glass transition could confirm the hypothesis that mechanical behavior is linked with the molecular dynamics in this adhesive.

CONCLUSION

This study points out that the use of dielectric spectroscopy is useful to analyze adhesive bonds. The broad frequency range and the service configuration analyze, i.e. as an adhesive joint, are advantageous. We access the molecular mobility in a configuration similar to classical mechanical tests. The study of hydrothermal effect on bonded assemblies at macroscopic and molecular scales is done. This study allows us to define β_1 relaxation mode as a pertinent aging parameter. The shear rupture stress decreases while the relaxation times associated with β_1 relaxation mode increases. Their evolutions show that water into the joint is a crucial parameter of hydrothermal aging as expected. It invites to be sure that hydroxyether moieties are linked with β_1, and to study the relationships between water–hydroxyether interactions and mechanical behavior. This result shows that at localized scale, water can act as an aging factor.

The correlation between real aging and accelerated results presented in this article will be completed in a future study. In the same time, real aging influence is analyzed. Mechanical and dielectric behavior are monitored. After 3 years of storage in spacecraft manufacturing conditions, the same parameters, i.e. the relaxation times of β_1 and the shear rupture stress, begin to evolve. The study will now focus on the correlation between these different aging conditions.

References

1. European Cooperation for space Standardization, Thermal testing for the evaluation of space materials, processes, mechanical parts and assemblies, ESA standard document, ECSS-Q-ST-70–04C, 2008.
2. Bellenger, V.; Verdu, J.; Morel, E. J Mater Sci 1989, 24, 63.
3. Apicella, A.; Nicolais, L.; De Castaldis, C. Adv Polym Sci 1985, 66, 189.
4. Gupta, V. B.; Drzal, L. T.; Lee, C. Y.-C.; Rich, M. J. Polym Eng Sci 1985, 25, 812.
5. Mijovic, J.; Zhang, H. Macromolecules 2003, 36, 1279.
6. Luo, S.; Leisen, J.; Wong, C. P. J Appl Polym Sci 2002, 85, 1.
7. Moy, P.; Karasz, F. E. Polym Eng Sci 1980, 20, 315.
8. Colombini, D.; Martinez-Vega, J. J.; Merle, G. Polymer 2002, 43, 4479.
9. Nogueira, P.; Ramirez, C.; Torres, A.; Abad, M. J.; Cano, J.; Lopez, J.; Lopez-Bueno, I.; Barral, L. J Appl Polym Sci 2001, 80, 71.
10. Comrie, R.; Affrossman, S.; Hayward, D.; Pethrick, R. A. J Adhes 2002, 78, 967.
11. Dodiuk, H.; Drori, L.; Miller, J. J Adhes 1984, 17, 33.
12. Bershtein, V. A.; Peschanskaya, N. N.; Halary, J. L.; Monnerie, L. Polymer 1999, 40, 6687.
13. Boye, J.; Demont, P.; Lacabanne, C. J Polym Sci Part B: Polym Phys 1994, 32, 1359.
14. Pangrle, S.; Wu, C. S.; Geil, P. H. Polym Compos 1989, 10, 173.
15. Ochi, M.; Kageyama, H.; Shimbo, M. Polymer 1988, 29, 320.
16. Maggana, C.; Pissis, P. J Macromol Sci Phys 1997, B36, 749.
17. Havriliak, S.; Negami, S. J Polym Sci Part C: Polym Symp 1966, 14, 99.
18. Havriliak, S.; Negami, S. Polymer 1967, 8, 161.
19. Buch, X. Ph.D. Thesis, Ecole des Mines de Paris, 2000.
20. Hedvig, P. Dielectric Spectroscopy of Polymers; Adam Hilger Ltd: Bristol, 1977.
21. Cognard, J. J Adhes 1994, 47, 43.